International Journal of Automotive Technology, Vol. 15, No. 7, pp. 1155–1164 (2014)
DOI 10.1007/s12239–014–0120–9

pISSN 1229–9138/ eISSN 1976–3832

MODEL PREDICTIVE CONTROL STRATEGY FOR SMOOTH PATH TRACKING OF AUTONOMOUS VEHICLES WITH STEERING ACTUATOR DYNAMICS

E. KIM[1)], J. KIM[2)] and M. SUNWOO[3)*]

[1)]Central R&D Center, Mando Corporation, 21 Pangyo-ro, 255 Beon-gil, Bundang-gu, Seongnam-si, Gyeonggi 463-400, Korea
[2)]Department of Automotive Engineering, Graduate School, Hanyang University, Seoul 133-791, Korea
[3)]Department of Automotive Engineering, Hanyang University, Seoul 133-791, Korea

(Received 17 July 2013; Revised 9 November 2013; Accepted 16 December 2013)

ABSTRACT–Path tracking control is one of the most important functions for autonomous driving. In path tracking control, high accuracy and smooth tracking are required for safe and comfort driving. In order to meet these requirements, model predictive control approaches, which can obtain an optimized solution with respect to a predefined path, have been widely studied. Conventional predictive controllers have been studied based on a simple bicycle model. However, the conventional predictive controllers have a performance limitation in practical challenges due to the difference between the simple bicycle model and the actual vehicle. To overcome this limitation, the actuator dynamics of the steering system should be incorporated into the control design. In this paper, we propose a model predictive control based path tracking control algorithm to achieve the accurate and smooth tracking by incorporating the dynamic characteristics of the steering actuation system. In the proposed control algorithm, an optimal trajectory of the steering command is calculated by applying a quadratic programming optimization method. The proposed controller was verified by computer simulation with various driving scenarios. The simulation results show that the proposed controller can improve the tracking performance.

KEY WORDS : Autonomous vehicle, Path tracking, Model predictive control, Vehicle control, Actuator dynamics

1. INTRODUCTION

Path tracking control is an essential function for an autonomous vehicle that guides the vehicle along a predefined path. The tracking must be accurate and smooth for safe driving, and must be robust in various driving conditions (Vahidi and Eskandarian, 2003). In order to meet these requirements, the control system should be eligible to deal with several vehicle characteristics, such as nonholonomic constraints (De Luca and Samson, 1998), vehicle dynamics (Rajamani, 2012), and physical limitations (e.g., constraints on the steering system, maximum allowable tire forces) (Zhu and Qzguner, 2008). In addition, the controller is required to solve a trade-off problem between tracking performance and ride comfort (Hemami and Mehrabi, 1997).

To deal with these vehicle characteristics, model predictive control (MPC) approaches are appropriate for several reasons. Firstly, the MPC method is applicable to the path tracking control where a future reference is provided from the predefined path. Secondly, the MPC method can easily handle the nonholonomic constraints due to its model-based design. The design process of the MPC method can then incorporate the physical limitations of the vehicle system as constraints. Lastly, an optimization technique of the MPC method can solve the trade-off problem between tracking performance and ride comfort.

Due to these advantages, many researchers have studied MPC method for path tracking control. The first attempt to apply the MPC approach in path tracking was performed by researchers at Carnegie Mellon University (Ollero and Amidi, 1991). A nonlinear MPC approach was proposed for path tracking control (Borrelli *et al*., 2005; Keviczky *et al*., 2006). Since linearization of the nonlinear prediction model may be able to generate errors, a linear time-varying MPC approach was proposed for the path tracking control (Katriniok and Abel, 2011). These studies used only a simple vehicle model and assumed that the dynamics of a steering system is negligible. However, the steering actuator dynamics cannot be negligible because it greatly affects the vehicle dynamics in the practical challenges.

This paper presents an MPC-based path tracking algorithm incorporating steering actuator dynamics and constraints. The proposed algorithm derives an optimal steering trajectory to solve the path tracking problem by using a quadratic programming (QP) optimization method.

**Corresponding author.* e-mail: msunwoo@hanyang.ac.kr

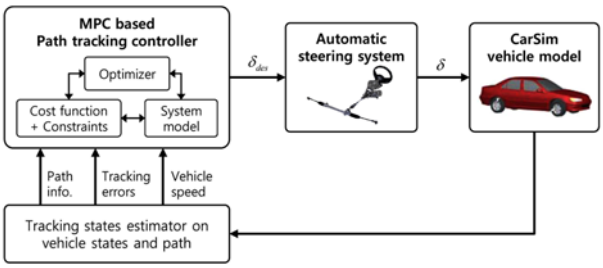

Figure 1. System architecture.

The proposed controller was validated and analyzed through simulations.

This paper is organized as follows: Chapter 2 describes the system architecture of the proposed controller. A system model of the controller and its dynamic equations is derived in Chapter 3. Chapter 4 explains the design process of the MPC-based path tracking control algorithm. In Chapter 5, simulation results are presented. Finally, Chapter 6 discusses the conclusions.

2. SYSTEM ARCHITECTURE

Figure 1 shows the system architecture of the predictive path tracking control. A predefined path, tracking errors, and vehicle speed are provided as input variables to the control system. With the input variables, the proposed controller determines a desired steering angle for the automatic steering system. The controller consists of four components: a system model, a cost function, constraints, and an optimizer. The system model is a combination of two simplified dynamic models: a steering dynamic model and a vehicle dynamic model. Based on the system model, the path tracking problem is formulated as a cost function. The constraints then represent the physical limitations of the vehicle systems. The QP optimization method is applied as an optimizer that can minimize the cost function subject to the constraints. Consequently, by using these components the controller can predict the vehicle trajectory and determine the optimal control input sequence.

3. MODELING

This chapter presents the modeling of the steering dynamics and vehicle dynamics in Sections 3.1 and 3.2, respectively. These two models are combined into an integrated model, which is described in Section 3.3. The integrated model is validated in Section 3.4 and applied to the control design as a system model in Chapter 4.

3.1. Steering Model

The steering model of the control design has two requirements. One is that the model should represent the actual system in the operation range. The other is that the model should be simple in the MPC method for less computational load. In order to obtain the steering model that satisfies the requirements, a frequency analysis is performed with four candidate models. These models are simple dynamic models (1st, 2nd, 3rd, and 4th order dynamic models) as depicted in Figure 2. These are developed from the simplification of the automatic steering system dynamics by using the prediction-error minimization (PEM) method of system identification (Ljung, 2002). Figure 3 illustrates a schematic of the identification.

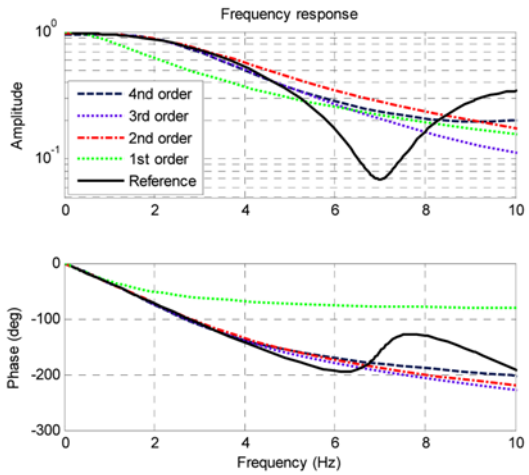

Figure 2. Frequency responses of the system.

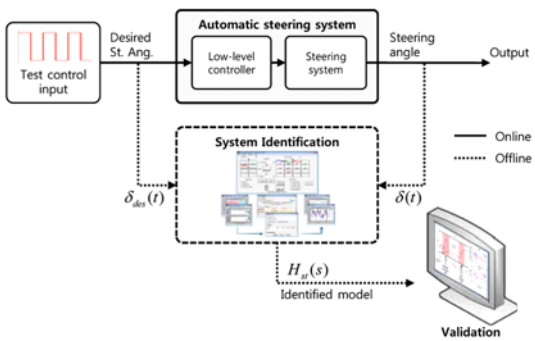

Figure 3. System identification schematic.

In Figure 2, the simplified models (except the first order) behave similarly to the reference model at frequencies from 0 Hz to 5 Hz. Since the frequency range covers the bandwidth of the steering system (3 Hz), these simplified models (except the first order) can represent the steering model. In order to meet the second requirement, the second order model is selected for the steering model of the controller. The comparison of the dynamic models of steering system in model predictive control is explained in the section 5.2.

Finally, the steering model is expressed as:

$$\frac{\delta}{\delta_{des}} = \frac{c_{st1}s + c_{st0}}{s^2 + a_{st1}s + a_{st0}} \tag{1}$$

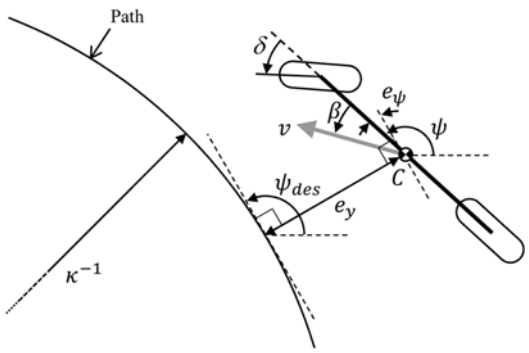

Figure 4. Definition of the tracking errors on the path.

where the input δ_{des} is the desired steering angle, and the output δ is the steering angle.

3.2. Vehicle Model

In this paper, a two degree-of-freedom (DOF) vehicle dynamic model (from Rajamani, 2012) is applied to the control design in which the state variables are defined in terms of position and orientation error with respect to the path. The first error variable e_y is the distance of the CG of the vehicle from the path. The second error variable e_ψ is the orientation error of the vehicle with respect to the path. Using a simplified vehicle model and tracking error variables as shown in Figure 4, the state space equation of the vehicle dynamic model is formulated as follows:

$$\begin{bmatrix} \dot{e}_y \\ \ddot{e}_y \\ \dot{e}_\psi \\ \ddot{e}_\psi \end{bmatrix} = \begin{bmatrix} 0 & 1 & 0 & 0 \\ 0 & a_{ve22} & a_{ve23} & a_{ve24} \\ 0 & 0 & 0 & 1 \\ 0 & a_{ve42} & a_{ve43} & a_{ve44} \end{bmatrix} \begin{bmatrix} e_y \\ \dot{e}_y \\ e_\psi \\ \dot{e}_\psi \end{bmatrix} + \begin{bmatrix} 0 \\ b_{ve21} \\ 0 \\ b_{ve41} \end{bmatrix} \delta + \begin{bmatrix} 0 \\ b_{ve22} \\ 0 \\ b_{42} \end{bmatrix} \omega_{des} \tag{2}$$

where ω_{des} is the derivative of the desired yaw angle, and

$$a_{ve22} = -\frac{2(c_f + c_r)}{m v_x}, \quad a_{ve23} = \frac{2(c_f + c_r)}{m},$$
$$a_{ve24} = -\frac{2(l_f c_f - l_r c_r)}{m v_x}, \quad a_{ve42} = \frac{2(l_f c_f - l_r c_r)}{I_z v_x},$$
$$a_{ve43} = \frac{2(l_f c_f - l_r c_r)}{I_z}, \quad a_{ve44} = -\frac{2(l_f^2 c_f + l_r^2 c_r)}{I_z v_x},$$
$$b_{ve21} = \frac{2c_f}{m}, \quad b_{ve41} = -\frac{2l_f c_f}{I_z},$$
$$b_{ve22} = -v_x - \frac{2(l_f c_f - l_r c_r)}{m v_x}, \quad b_{ve42} = -\frac{2(l_f^2 c_f + l_r^2 c_r)}{I_z v_x},$$

where c_f and c_r are the cornering stiffness of front and rear tires, l_f and l_r are the distance of the CG of the vehicle front and rear axles, and m and I_z are called the vehicle mass and the yaw moment of inertia.

3.3. Model Integration

Since the steering dynamics are coupled with the vehicle dynamics in the vehicle system, both dynamics are mathematically integrated into the system model of the path tracking controller. The integrated model is derived from the steering model and the vehicle model in Equations (1) and (2), respectively, as follows:

$$\begin{bmatrix} \dot{e}_y \\ \ddot{e}_y \\ \dot{e}_\psi \\ \ddot{e}_\psi \\ \dot{x}_{st1} \\ \dot{x}_{st2} \end{bmatrix} = \begin{bmatrix} 0 & 1 & 0 & 0 & 0 & 0 \\ 0 & a_{ve22} & a_{ve23} & a_{ve24} & b_{ve21}c_{st0} & b_{ve21}c_{st1} \\ 0 & 0 & 0 & 1 & 0 & 0 \\ 0 & a_{ve42} & a_{ve43} & a_{ve44} & b_{ve41}c_{st0} & b_{41}c_{st1} \\ 0 & 0 & 0 & 0 & 0 & 1 \\ 0 & 0 & 0 & 0 & -a_{st0} & -a_{st1} \end{bmatrix} \begin{bmatrix} e_y \\ \dot{e}_y \\ e_\psi \\ \dot{e}_\psi \\ x_{st1} \\ x_{st2} \end{bmatrix} + \begin{bmatrix} 0 \\ 0 \\ 0 \\ 0 \\ 0 \\ 1 \end{bmatrix} \delta_{ref} + \begin{bmatrix} 0 \\ b_{ve22} \\ 0 \\ b_{ve42} \\ 0 \\ 0 \end{bmatrix} \omega_{des} \tag{3}$$

where x_{st1} and x_{st2} are the angular position and velocity of the steering system, and $\{\cdot\}_{st}$ and $\{\cdot\}_{ve}$ denote the elements of the steering model and vehicle model, respectively.

3.4. Model Validation

The integrated model in Equation (3) is validated with the reference steering model and the CarSim vehicle model. The validation is performed on a flat road at different speeds. Figure 5 illustrates the structure of the validation. In the validation process, the sinusoidal control input in Figure 6 is applied to both the reference model and the integrated model, and the outputs of the models are then compared.

Figures 7 and 8 show the validation results at 20 km/h and 40 km/h, respectively. The integrated model behaves similarly to the reference system in terms of lateral position and orientation. The model accuracy decreases at high speed.

In order to evaluate the model accuracy in various driving conditions, more tests are performed at different vehicle speeds from 10 km/h to 60 km/h, and at different amplitudes of sinusoidal control inputs from 5 degrees to 30 degrees. The contour plots in Figure 9 and 10 show the RMS errors of lateral position and orientation, respectively.

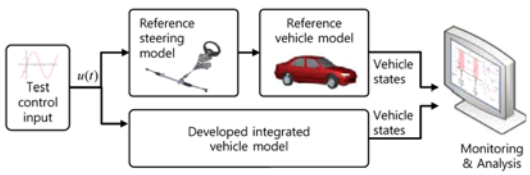

Figure 5. Validation structure of the integrated model.

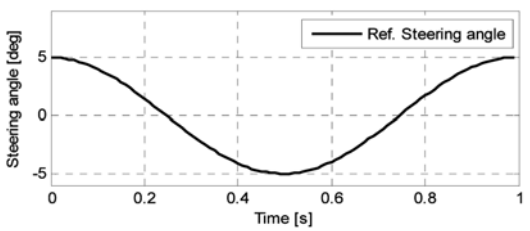

Figure 6. Desired steering angle for the validation.

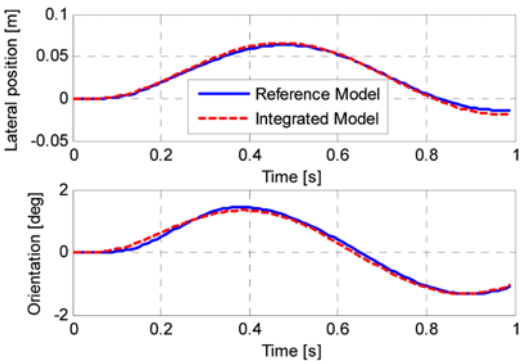

Figure 7. Model validation results at 20 km/h.

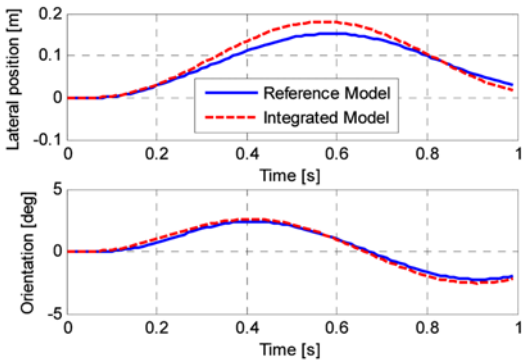

Figure 8. Model validation results at 40 km/h.

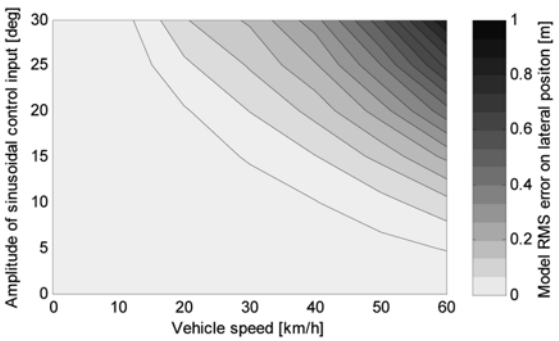

Figure 9. Tracking RMS errors of position.

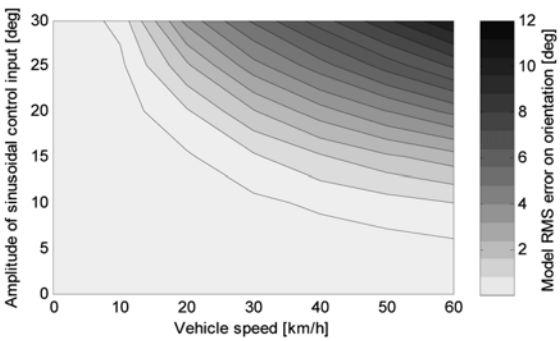

Figure 10. Tracking RMS errors of orientation.

The region of large position errors in Figure 9 (over about 0.1 m) should be avoided for safety in autonomous driving. The integrated model can then represent an actual vehicle in normal driving conditions.

4. CONTROL DESIGN FOR PATH TRACKING

This section introduces the control design procedure for solving the proposed path tracking problem and the problems caused by the steering actuator. In the control design, these problems are formulated as a constrained optimization problem. The QP method is applied to solve the optimization problem. The predefined path, tracking states, and vehicle states are provided to determine the desired steering angle for the automatic steering system.

In the following formulation, N_c denotes the length of the control horizon and N_p denotes the length of the prediction horizon. $\{\cdot\}(k_i+j|k_i)$ and $\{\cdot\}(k_i+j)$ denote the prediction and future control, respectively, at initial time k_i of the variable $\{\cdot\}$ at predicted time k_i+j.

In path tracking, there is a trade-off between control input and tracking performance. In order to balance the trade-off, an optimization technique is applied over the prediction horizon. The trade-off is defined as the cost function in the form of a quadratic equation as follows:

$$J = Y^T \bar{Q} Y + \Delta U^T \bar{R} \Delta U = \sum_{k=k_i}^{k_i+N_p} y_{k|k_i}^T \bar{q} y_{k|k_i} + r_w \sum_{k=k_i}^{k_i+N_c-1} \Delta u_k^2 \quad (4)$$

where Y and ΔU are given by

$$Y = \begin{bmatrix} y(k_i+1|k_i) \\ y(k_i+2|k_i) \\ \vdots \\ y(k_i+N_p|k_i) \end{bmatrix}, \quad \Delta U = \begin{bmatrix} \Delta u(k_i) \\ \Delta u(k_i+1) \\ \vdots \\ \Delta u(k_i+N_c-1) \end{bmatrix}$$

$y(k|k_i) = [e_y(k|k_i)\ \Delta e_y(k|k_i)\ e_\psi(k|k_i)\ \Delta e_\psi(k|k_i)]$, $k = k_i, k_i+1, k_i+2, \ldots, k_i+Np$ are the system outputs that contain tracking errors in the position and orientation at each prediction horizon. $\Delta u(k_i+j) = u(k_i+j) - u(k_i+j-1)$, $j = 0, \ldots, N_c - 1$ are the incremental control inputs which represent the desired steering angle δ_{des} at time k. $\bar{Q}$ is a diagonal matrix consisting of the set of $\bar{q}$ in Equation (5). A weighting factor q is for balancing between the tracking errors in lateral position and orientation. $\bar{R}$ is a weighting factor between the tracking errors and the control input as shown in Equation (6). In order to decouple the control effort from the variation of the prediction horizon N_p, Equation (7) shows the tuning parameter r_w that is defined as a function of the prediction horizon.

$$\bar{Q} = \underbrace{\begin{bmatrix} \bar{q} & 0 & \cdots & 0 \\ 0 & \bar{q} & \cdots & 0 \\ \vdots & \vdots & \ddots & 0 \\ 0 & 0 & 0 & \bar{q} \end{bmatrix}}_{4N_p} \quad where \quad \bar{q} = \begin{bmatrix} 1 & 0 & 0 & 0 \\ 0 & 1 & 0 & 0 \\ 0 & 0 & q & 0 \\ 0 & 0 & 0 & q \end{bmatrix} \quad (5)$$

$$\bar{R} = r_w \cdot I_{N_c \times N_c}, \tag{6}$$

$$r_w = rN_p \tag{7}$$

This research considers two limitations of the control design. The first limitation is the physical limitations of the steering system. If the control input command exceeds the limitation, the system model is no longer valid and the actuator system might perform an unstable operation. The other is the steering angle limitation for safe driving according to the vehicle speed. The steering angle limitation is derived from the kinematic relationship between the steering angle and the road curvature. The angle limitation is determined by a base lateral acceleration $a_{y,\text{base}}$ with a steering margin δ_{margin} at the vehicle speed v_x. By limiting the steering angle according to vehicle speed, the controller not only provides safe driving, but also guarantees high model accuracy with the linear dynamic vehicle model.

Consequently, both limitations are applied to the constraints on the steering angle amplitude, which are defined as functions of vehicle speed v_x as written in (8).

$$\begin{aligned} u_{\max}(v_x) &= \begin{cases} \delta_{\max} & when \quad \eta_{\max}(v_x) \geq \delta_{\max} \\ \eta_{\max}(v_x) & when \quad \eta_{\max}(v_x) < \delta_{\max} \end{cases} \\ u_{\min}(v_x) &= \begin{cases} -\delta_{\max} & when \quad \eta_{\max}(v_x) \geq \delta_{\max} \\ -\eta_{\max}(v_x) & when \quad \eta_{\max}(v_x) < \delta_{\max} \end{cases} \end{aligned} \tag{8}$$

where $\eta_{\max}(v_x) = \dfrac{l}{v_x^2} a_{y,\text{base}} + \delta_{\text{margin}}$ (9)

$\delta_{\max}$ is the maximum physical steering angle, l is the wheelbase of the vehicle ($l = l_f + l_r$), and $\eta_{\max}(v_x)$ is the steering angle limitation at vehicle speed v_x. The shaded area in Figure 11 depicts the allowable region of the steering angle under the constraints.

In the control design, the rate saturation of the steering system is also considered as a constraint. The constraint is defined by the steering angle limitation $u_{\max}$ with the bandwidth of the steering model ω_{BW}. The rate limitation is the maximum rate of the sinusoidal input of the steering angle limitation at the bandwidth frequency. The sinusoidal input is given by:

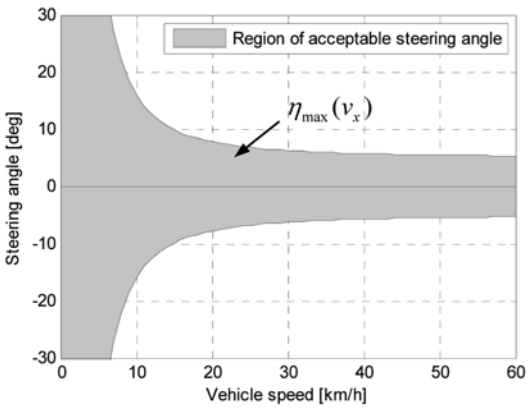

Figure 11. Region of constrained control input.

$$u(\omega, t) = A \sin\ \omega t \tag{10}$$

$$\dot{u}(\omega, t) = A\omega\ \cos\ \omega t \tag{11}$$

The maximum rate at the bandwidth frequency is

$$max\ |\dot{u}(\omega_{BW}, t)| = A\omega_{BW} \tag{12}$$

At high speed the amplitude of the control input is limited by the constraint in Equation (8). Therefore, the upper and lower limitations of the incremental variation at the sampling period T_s are defined as a function of the amplitude limitation of the control input as follows:

$$\begin{aligned} \Delta u_{\max} &= u_{\max}(v_x)\omega_{BW} T_s \\ \Delta u_{\min} &= u_{\min}(v_x)\omega_{BW} T_s \end{aligned} \tag{13}$$

Finally, the defined constraints are applied to the control design in the form of the inequality function at sample time k_i, as shown in Equation (14):

$$\begin{aligned} u_{\min} &\leq u(k_i + j) \leq u_{\max} \\ \Delta u_{\min} &\leq \Delta u(k_i + j) \leq \Delta u_{\max} \end{aligned} \tag{14}$$

where $j = 0, \ldots, N_c - 1$

Note that the constraints are considered in every future sample, and the optimal steering sequence is derived from the integrated model by minimizing the cost function with the constraints.

The difficulty is in the minimization of the quadratic cost function (4) whose variables are subject to the linear inequality constraints (14). In order to solve the optimal problem with constraints, Karush-Kuhn-Tucker (KKT) conditions and Hildreth's QP procedure (from Wang, 2009) are applied.

5. SIMULATION RESULTS

This chapter presents the simulation results of the proposed controller. In order to evaluate the controller, three simulation scenarios are demonstrated. First, the effect of the varying prediction horizon was analyzed and the appropriate length of the prediction horizon was determined. Control ability was then analyzed according to vehicle speed. Lastly, the effectiveness of the controller was validated with the MPC-based path tracking controller, which does not include the actuator dynamics and constraints.

5.1. Simulation Environments

In order to validate the proposed controller, a mathematical model of an automatic steering system and the 27 degree-of-freedom CarSim vehicle model are applied as reference systems. The automatic steering model is developed by modeling the electric motor dynamics and the mechanical

dynamics of the steering system. More details about the reference steering model are introduced in the Appendix. The reference vehicle model is provided from CarSim software. CarSim software has nonlinear vehicle models of actual vehicles for vehicle dynamic simulation.

The three simulation scenarios are demonstrated on two different roads: a double lane change (DLC) course and a road course. Figure 12 illustrates the DLC course that is a straight section of two lane road. This course demonstrates the tracking capability in different prediction horizons and controller validation. The road course is depicted in Figure 13 and it facilitates a general performance comparison. This course is used for controller validation at different speeds.

In the simulation, the vehicle speed is constant, the road is flat, and the predefined path is continuous, but the curvature of the path is discontinuous. The control system operates at 100 Hz and the simulation operates at 1 kHz. The control parameters for simulations are denoted in Table 1.

5.2. Effect of Model Order of Steering System

The model order of steering system for the model predictive controller should be appropriate value. A low order system provides less accuracy, and a high order system provides high accuracy but it brings large computation time. The model order of steering system is analyzed in frequency domain in section 3.1. In order to check the feasibility of the selection in section 3.1, the steering models are compared in terms of the model predictive control. The simulation is performed with 1st, 2nd, and 3rd order transfer functions of steering system at 40 km/h, and its results are shown in Figure 14.

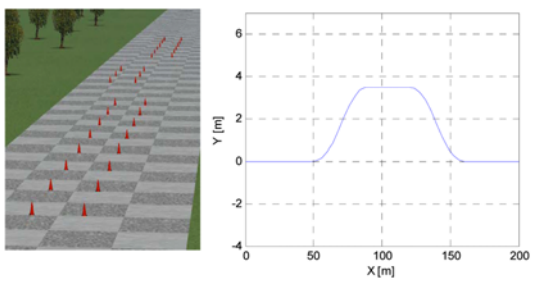

Figure 12. Double lane change course.

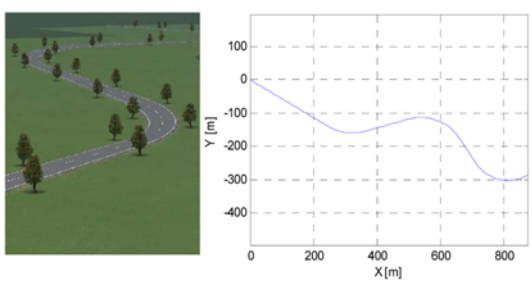

Figure 13. Road course.

Table 1. Control parameters for the simulation.

Description	Notation	Value
Prediction horizon length	N_p	20
Control horizon length	N_c	8
Sampling interval of the controller	T_s	10 ms
Weighting factor between the errors on lateral position and orientation	q	0.5
Weighting factor between the tracking errors and the control input	r	60
Base lateral acceleration	$a_{y,base}$	0.5 m/s^2
Steering margin	δ_{margin}	5°

While the tracking results of using the 2nd and 3rd order steering models are quite good, the tracking result of using the 1st order model shows worse tracking performance and brings large oscillation on the driving. The 2nd order dynamic model of steering system is the lowest order model that can provide good tracking results. From the simulation results, the order selection in section 3.1 is verified.

5.3. Effect of Prediction Horizon

The first scenario is performed to analyze the effect of prediction horizon length and to find the proper value of the horizon length of the proposed controller. The simulations were performed on the DLC course at 40 km/h with different prediction horizon lengths (N_p = 8, 12, 20,

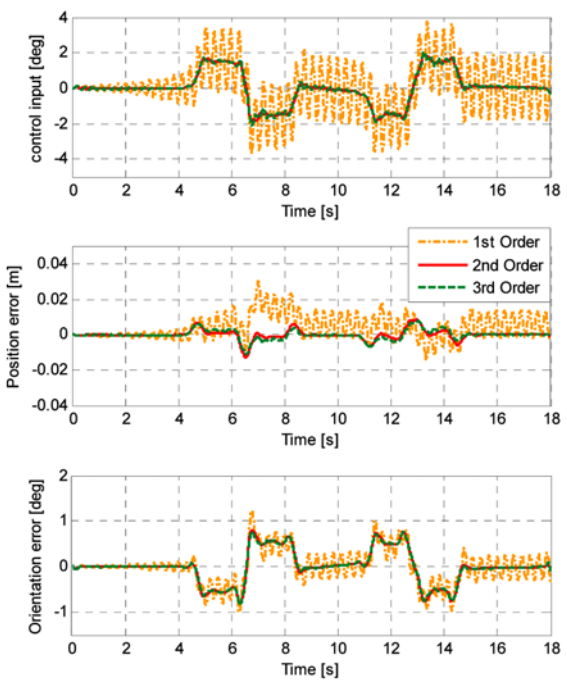

Figure 14. Tracking results with different model order of steering system.

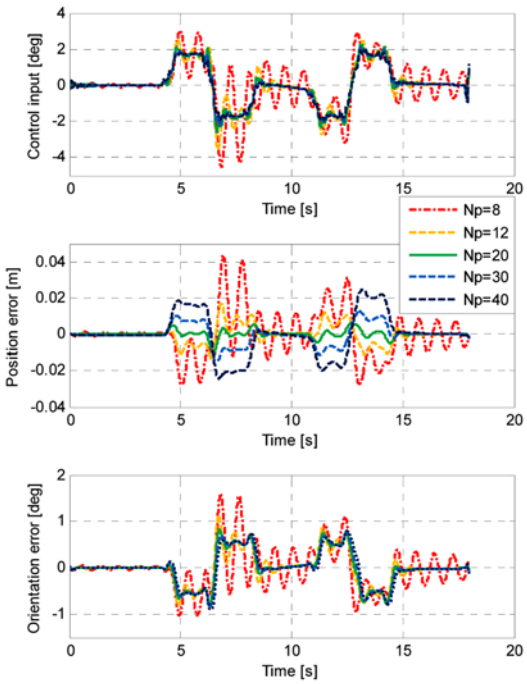

Figure 15. Tracking results with different prediction horizons.

30, and 40). Figure 15 shows the simulation results.

The results show that the vehicle oscillates during driving at $N_p = 8$, since the prediction horizon is insufficient to cover the actuator dynamics. At horizon lengths less than 20 the vehicle trajectory overshoots the predefined path after the turn, whereas at horizon lengths greater than 20 the vehicle makes anticipated moves before the turn. The anticipated move is the optimization results from the MPC-based controller minimizing tracking errors over the entire horizon. The driving with a large horizon length brings the similar results with the driving with gazing into a far distance. Therefore it provides relatively stable driving but provides larger tracking error at the current vehicle position. In order to balance between driving stability and tracking error, an appropriate horizon length should be

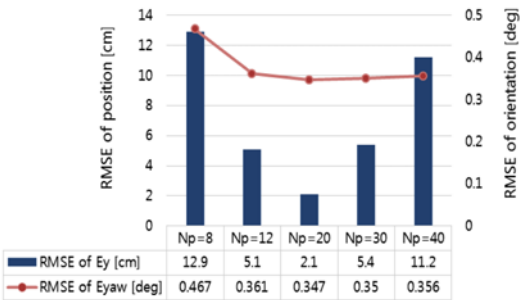

Figure 16. RMS tracking errors in position and orientation for different prediction horizon lengths.

Table 2. Average computation time for the proposed controller.

Description	Time/call
MPC controller with $N_c = 8$, $N_p = 8$	2.66 ms
MPC controller with $N_c = 8$, $N_p = 12$	3.31 ms
MPC controller with $N_c = 8$, $N_p = 20$	3.42 ms
MPC controller with $N_c = 8$, $N_p = 30$	4.86 ms
MPC controller with $N_c = 8$, $N_p = 40$	4.97 ms

selected.

Figure 16 illustrates bar graphs depicting the tracking RMS errors in position and orientation for the whole simulation at the different horizon lengths ($N_p = 8$, 12, 20, 30, and 40). The lateral position error is smallest at $N_p = 20$. Thus, the prediction horizon length of 20 is regarded as a proper value in the proposed controller.

Table 2 shows the average computation time for the proposed controller. The computation is performed with 2.4 GHz of Intel® quad-core CPU. Since the sampling interval is 10 ms, the all performed MPC controllers have acceptable computation times.

5.4. Performance Evaluation of the Proposed Controller

In order to evaluate the tracking performance of the proposed controller according to vehicle speed, the last scenario is performed on the road course with different constant velocities of 20, 40, 60, and 80 km/h. Each simulation took about 180, 120, 90, and 45 seconds, respectively. Figure 17 shows the simulation results.

Tracking errors are small even at high speeds. In the

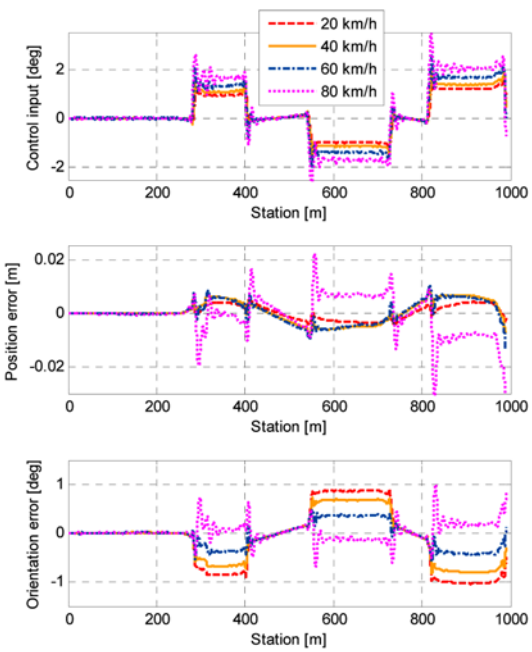

Figure 17. Tracking results at different speeds.

simulation, the maximum tracking errors in position and orientation are under 4 cm and 1 degree, respectively. Note that the position tracking errors at different speeds are almost identical, which confirms that the proposed controller satisfies the acceptable tracking performance at various vehicle speeds under the actuator dynamics and its constraints.

5.5. Comparison Result

In order to validate the proposed controller, two different controllers are applied in the second scenario. Case A is the proposed controller, which is the MPC-based path tracking controller that incorporates actuator dynamics and constraints. Case B is the MPC-based path tracking controller based solely on the vehicle dynamics model. Both controllers use the parameters delineated in Table 1.

The first simulation of both controllers was performed at 20 km/h, and its results are shown in Figure 18. Case B shows small oscillation in the driving, which is not a big problem in terms of driving stability. However, the oscillation increases as the vehicle speed increases, and the system would be unstable at higher speeds. Figure 19 illustrates the simulation results at 40 km/h. In this simulation, Case B shows large oscillations in the driving.

The controller that does not consider actuator dynamics shows worse control performance as speed increases. On the other hand, the proposed controller maintains high tracking performance even at high speeds.

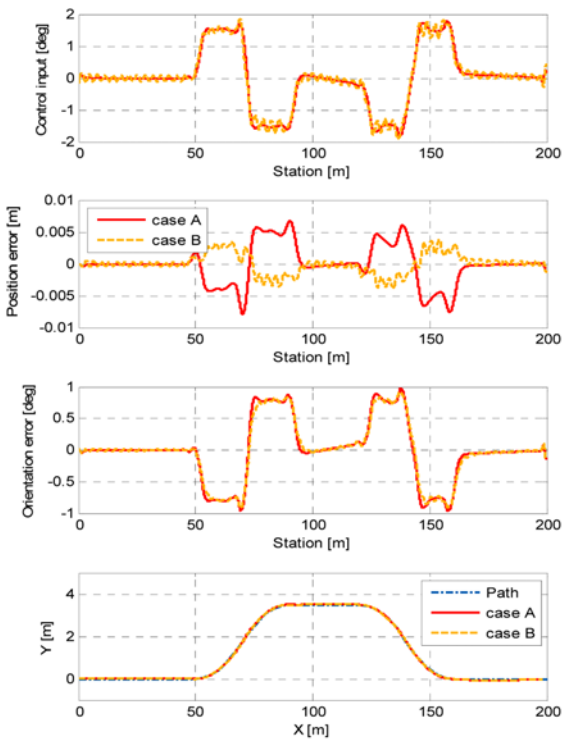

Figure 18. Simulation results on the DLC at 20 km/h.

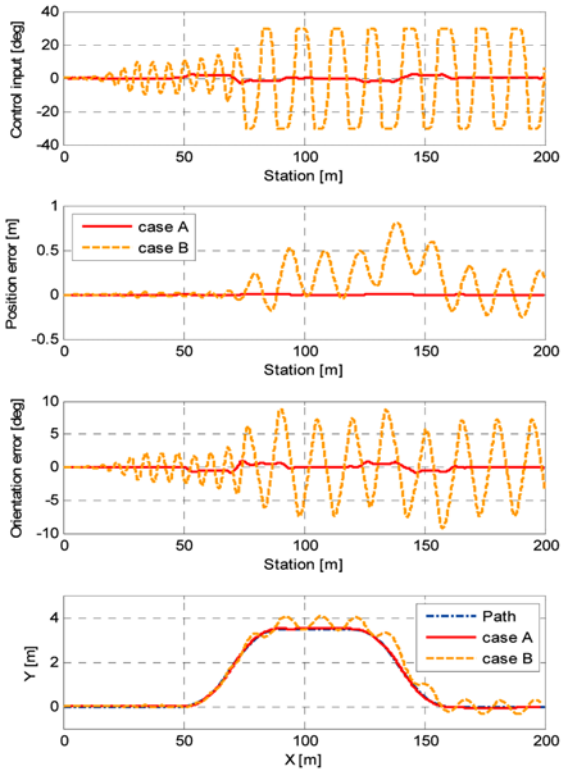

Figure 19. Simulation results on the DLC at 40 km/h.

6. CONCLUSION

In this paper, a model predictive control based path tracking algorithm was proposed to achieve an accurate and smooth tracking for an autonomous vehicle. In the control design of the proposed controller, dynamic characteristics of the steering system were incorporated to improve the tracking performance by integrating with vehicle model into an integrated model. An optimal steering command was calculated by using a QP optimization method based on the integrated model. The integrated model was validated under various driving conditions. In addition, high model accuracy and safe driving were ensured by applying different limitations on the steering angle according to vehicle speed.

The performance of the proposed algorithm was validated through various simulations. According to the simulation results, the length of the prediction horizon should be long enough to compensate the steering actuator dynamics. In comparing the proposed controller to another controller based only on the vehicle dynamics model, the proposed controller showed better tracking performance by incorporating the steering actuator dynamics, especially at the high speed. In conclusion, the simulation results confirmed that the proposed control algorithm achieves not only high tracking accuracy but also driving smoothness.

ACKNOWLEDGEMENT–This work was supported by an NRF

grant funded by the Korean government (MEST) (No. 2011-0017495), Industrial Strategy Technology Development Program of MKE (No. 10039673), Energy Resource R&D program (2006ETR11P091C) under the MKE, the BK21 plus Program (22A20130000045) under the Ministry of Education, and MKE and KIAT through the Workforce Development Program in Strategic Technology.

REFERENCES

De Luca, G. O. A. and Samson, C. (1998). Feedback control of a nonholonomic car-like robot. *Robot Motion Planning and Control*, 171–249.

Borrelli, F., Falcone, P., Keviczky, T., Asgari, J. and Hrovat, D. (2005). MPC-based approach to active steering for autonomous vehicle systems. *Int. J. Vehicle Autonomous Systems* **3**, **2**, 265–291.

Hemami, A. and Mehrabi, M. (1997). On the steering control of automated vehicles. *Intelligent Transportation System, ITSC '97, IEEE Conf.*, 266–271.

Katriniok, A. and Abel, D. (2011). LTV-MPC approach for lateral vehicle guidance by front steering at the limits of vehicle dynamics. *Decision and Control and European Control Conf. (CDC-ECC), 2011 50th IEEE Conf.*, 6828–6833.

Keviczky, T., Falcone, P., Borrelli, F., Asgari, J. and Hrovat, D. (2006). Predictive control approach to autonomous vehicle steering. *American Control Conf.*

Ljung, L. (2002). Prediction error estimation methods. *Circuits, Systems and Signal Processing*, **21**, 11–21.

Ollero, A. and Amidi, O. (1991). Predictive path tracking of mobile robots. Application to the CMU NavLab. *Advanced Robotics, 'Robots in Unstructured Environments', 91 ICAR., 5th Int. Conf.*, **2**, 1081–1086.

Rajamani, R. (2012). *Vehicle Dynamics and Control.* Springer. Berlin.

Vahidi, A. and Eskandarian, A. (2003). Research advances in intelligent collision avoidance and adaptive cruise control. *Intelligent Transportation Systems, IEEE Trans.*, **4**, 143–153.

Wang, L. (2009). *Model Predictive Control System Design and Implementation Using MATLAB®*. Springer. Berlin.

Zhu, Y. and Ozguner, U. (2008). Constrained model predictive control for nonholonomic vehicle regulation problem. *Proc. 17th IFAC World Cong.,* 9552–9557.

APPENDIX

This chapter presents the reference model of the automatic steering system for the simulations. In this study, the steering model is developed over two steps. First, the electric motor dynamics and the mechanical dynamics of the steering system are modeled as a steering plant model. Then, a simple PID control law is applied to the steering system with an input voltage limitation.

Figure A illustrates the structure of the automatic steering system. The steering system consists of an electric motor, steering wheel, steering column, rack, and wheel. In order to develop the steering model, we assume that there is no driver intervention on the steering wheel and that the rack position is proportional to the steering angle. In accordance with Newton's laws of motion, we derived the following motion equations.

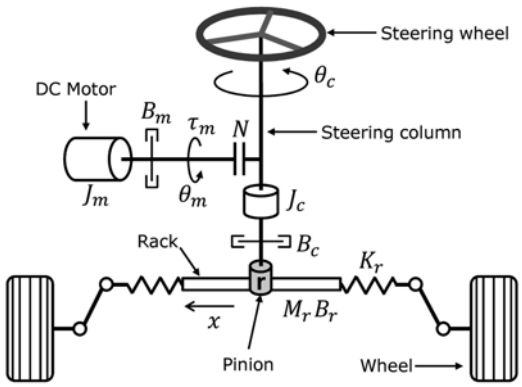

Figure A. Automatic steering mechanism.

The electric motor dynamics is given by:

$$\tau_m = k_t i \tag{1}$$

$$L\frac{di}{dt} + Ri = v - k_t \dot{\theta}_m \tag{2}$$

The dynamic equations of the mechanical parts are given by:

$$J_m\ddot{\theta}_m + B_m\dot{\theta}_m + K_m(\theta_m - N\theta_c) = \tau_m \tag{3}$$

$$J_c\ddot{\theta}_c + B_c\dot{\theta}_c + K_p\left(\theta_c - \frac{x}{r}\right) = NK_m(\theta_m - N\theta_c) \tag{4}$$

$$M_r\ddot{x} + B_r\dot{x} + K_r x = \frac{1}{r}K_p\left(\theta_c - \frac{x}{r}\right) - \frac{2\tau_s}{N_s} \tag{5}$$

$$\tau_s = \xi F_{yf} \tag{6}$$

where $\theta_m = N\theta_c$, $x = r\theta_c$, and $\delta = N_s x$ at steady-state. In the above equations, the meanings of the symbols involved are explained in Table A. From Equation (1), the motor torque τ_m is related to the armature current i by a constant factor k_t. In voltage Equation (2), the armature current i can be expressed in terms of the applied motor terminal voltage v by applying Kirchhoff's voltage law to the armature circuit. A back-EMF is related to the rotational velocity of the motor armature by the constant factor k_t. In Equations (3) and (4), Newton's laws of motion are applied to the angular motion on the motor armature and the steering column, respectively, in terms of the torque. Equation (5) shows forces on the steering rack by applying Newton's laws. Self-align torque on the front wheel is a function of lateral tire force with the pneumatic trail ξ in torque Equation (6). Therefore, the above equations present the physical mechanism by which electric motor generates torque and that torque is then transferred via the steering column and

the steering rack to the front wheel for steering.

Using Equations (1) through (6), the state-space form of dynamics model of the steering system can be derived as follows:

$$\begin{bmatrix} \dot{i} \\ \ddot{\theta}_m \\ \dot{\theta}_m \\ \ddot{\theta}_c \\ \dot{\theta}_c \\ \ddot{x} \\ \dot{x} \end{bmatrix} = \begin{bmatrix} a_{st11} & 0 & a_{st13} & 0 & 0 & 0 & 0 \\ a_{st32} & a_{st22} & a_{st23} & 0 & a_{st25} & 0 & 0 \\ 0 & 1 & 0 & 0 & 0 & 0 & 0 \\ 0 & 0 & a_{st43} & a_{st44} & a_{st45} & 0 & a_{st47} \\ 0 & 0 & 0 & 1 & 0 & 0 & 0 \\ 0 & 0 & 0 & 0 & a_{st65} & a_{st66} & a_{st67} \\ 0 & 0 & 0 & 0 & 0 & 1 & 0 \end{bmatrix} \begin{bmatrix} i \\ \dot{\theta}_m \\ \theta_m \\ \dot{\theta}_c \\ \theta_c \\ \dot{x} \\ x \end{bmatrix} + \begin{bmatrix} b_{st11} & 0 \\ 0 & 0 \\ 0 & 0 \\ 0 & 0 \\ 0 & 0 \\ 0 & b_{st62} \\ 0 & 0 \end{bmatrix} \begin{bmatrix} v \\ \tau_s \end{bmatrix} \tag{7}$$

$$\delta = N_s x \tag{8}$$

where $a_{st11} = -\frac{R}{L}$, $a_{st13} = -\frac{k_t}{L}$, $a_{st21} = -\frac{k_t}{J_m}$,

$a_{st22} = -\frac{B_m}{J_m}$, $a_{st23} = -\frac{K_m}{J_m}$, $a_{st25} = \frac{K_m N}{J_m}$,

$a_{st43} = \frac{NK_m}{J_c}$, $a_{st44} = -\frac{B_c}{J_c}$, $a_{st45} = -\frac{N^2 K_m + K_p}{J_c}$,

$a_{st47} = \frac{K_p}{J_c r}$, $a_{st65} = \frac{K_p}{M_r r}$, $a_{st66} = -\frac{B_r}{M_r}$,

$a_{st67} = -\frac{K_r r^2 + K_p}{M_r r^2}$, $b_{st11} = \frac{1}{L}$, $b_{st62} = -\frac{1}{M_r N_s}$,

Table A. Parameters and variables of the model.

Description	Symbol	Unit
Steering wheel(column) angle	θ_c	rad
Steering column moment of inertia	J_c	kg·m^2
Steering column damping	B_c	Nm/(rad/s)
Radius of pinion	r_p	m
Pinion and rack torsional stiffness	K_p	Nm/rad
Rack and wheel assembly mass	M_r	kg
Rack damping	B_r	N/(m/s)
Rack spring constant	K_r	N/m
Motor's angular position	θ_m	rad
Motor moment of inertia	J_m	kg·m^2
Motor damping	B_m	Nm/rad
Motor and gearbox torsional stiffness	K_m	Nm/rad
Motor electric torque	T_m	Nm
Motor gear ratio	N	-
Rack steering ratio	N_s	Rad/s
Rack displacement	x	m
Motor torque and voltage constant	k_t	Nm/A
Motor inductance	L	H
Motor resistance	R	Ω
Motor terminal voltage	v	V
Motor armature current	i	A